










Cite this: *RSC Adv.*, 2020, 10, 22257

Photodynamic properties of tungsten iodide clusters incorporated into silicone: $A_2[M_6I_8L_6]$ @silicone†

Thorsten Hummel, ^a Danuta Dutczak,^a Alexander Y. Alekseev, ^{bc} Lyubov S. Adamenko, ^b Michael A. Shestopalov, ^d Yuri V. Mironov, ^d David Enseling, ^e Thomas Jüstel ^e and Hans-Jürgen Meyer ^{*a}

The light-induced antibacterial and antifungal properties of $A_2[M_6I_8L_6]$ with $M = Mo$ and W , $A =$ organic cation, $L =$ ligand have been studied. The photoactive compounds $(TBA)_2[W_6I_8(C_7H_7SO_3)_6]$ and $(TBA)_2[W_6I_8(COOCF_3)_6]$ have been incorporated into a permeable silicone matrix and were measured for their application in the decomposition of multi-resistant bioactive species (hospital germs) such as *S. aureus* and *P. aeruginosa* as well as fungi. In addition, we present a new high volume synthesis route for these types of cluster compounds departing from the soluble compound W_6I_{22} .

Received 4th March 2020

Accepted 20th May 2020

DOI: 10.1039/d0ra04280c

rsc.li/rsc-advances

Introduction

A large number of binary tungsten iodide clusters has been recently reported, of which the well-known W_6I_{12} with an octahedral cluster core is the most stable one.¹ The connectivity between clusters in the layered structure of W_6I_{12} preclude its solubility and thus any solution chemistry, in contrast to the $[W_6I_{14}]^{2-}$ ion.

$A_2[W_6X_8X_6^a]$ type compounds with $A =$ organic cation, $X = Cl, Br$ and I were reported for their versatile photophysical properties.^{2–9} Their structures are based on an octahedral tungsten cluster with eight μ_3 -bridging (or $i =$ inner) and six terminal (or $a =$ outer) halide ligands over the corners of the cluster core.

Ligand substituted clusters of the type $A_2[W_6X_8L_6]$ with L being an organic or inorganic ligand, can be synthesized by ligand exchange reactions in solution, mostly performed with silver salts, e.g. $Ag(C_7H_7SO_3)$ to yield $A_2[W_6X_8(C_7H_7SO_3)_6]$.

Upon excitation by means of UV/vis radiation, all these clusters emit light with a broad emission band in the deep red region of the visible spectrum (650–700 nm). As a competing process, the luminescence (in fact phosphorescence) is quenched in the presence of molecular oxygen.¹⁰ The quenching process involves energy transfer from cluster triplet states to ground-state oxygen ($X^3\Sigma_g$). The quantum yield of the O_2 ($a^1\Delta_g$) emission can be determined *via* the characteristic 1275 nm phosphorescence.¹¹ The dependency of the photoluminescence intensity with the oxygen partial pressure is fully reversible, qualifying this material type to sense oxygen.^{12,13}

Similar properties are reported for basic compounds $A_2[W_6X_8X_6]$. However, they show luminescence quenching by molecular oxygen, respectively singlet oxygen generation in solution, but not in solid state. Among mixed $A_2[W_6X_8X_6]$ clusters with $X = Cl, Br, I$ the all-iodide compounds are of particular interest because they reveal the highest quantum yields.¹⁴

Preparations of $A_2[W_6X_8L_6]$ require several steps, following some standard procedures. The bottle neck of the reaction chain involves the transformation of (insoluble) $Cs_2[W_6I_8I_6]$ into $A_2[W_6I_8I_6]$ in which A typically is TBA (*n*-tetrabutylammonium). In this work we present a new synthesis route departing from W_6I_{22} , allowing for an efficient high-volume synthesis of $A_2[W_6I_8L_6]$ compounds.

These compounds as well as molybdenum analogues $A_2[Mo_6I_8L_6]$ have been subject of extensive research including phosphorescence,¹⁵ disinfection,¹⁶ photodynamic therapy¹⁷ and photodynamic reduction.^{18,19} The photodynamic inactivation of bacteria or cells is mostly limited by the poor cellular uptake without the use of carriers, but there is an emerging research to address this problem.²⁰

For antibacterial and antifungal studies performed in this work, compounds are incorporated into silicone matrices.

^aSection for Solid State and Theoretical Inorganic Chemistry, Institute of Inorganic Chemistry, University of Tübingen, Auf der Morgenstelle 18, 72076 Tübingen, Germany. E-mail: juergen.meyer@uni-tuebingen.de

^bFederal Research Centre for Basic and Translational Medicine, 2 Timakova St., 630090 Novosibirsk, Russia

^cDagestan State University, 43a Gadzhiev Street, 367000, Makhachkala, Dagestan, Russia

^dNikolaev Institute of Inorganic Chemistry SB RAS, 3 Acad. Lavrentieva, 630090 Novosibirsk, Russia

^eDepartment of Chemical Engineering, Münster University of Applied Science, Stegerwaldstraße 39, 48565 Steinfurt, Germany

† Electronic supplementary information (ESI) available: Fig. S1–S3; emission integrals and decay times of clusters incorporated into silicone. Fig. S4; X-ray pattern of W_6I_{22} . Fig. S5; photographs of microorganisms' growth in LB agar culture media. See DOI: 10.1039/d0ra04280c



Tungsten iodide compounds $(\text{TBA})_2[\text{W}_6\text{I}_8(\text{C}_7\text{H}_7\text{SO}_3)_6]$ and $(\text{TBA})_2[\text{W}_6\text{I}_8(\text{COOCF}_3)_6]$ are selected because their photo-physical properties were well studied and they are known to behave sufficiently stable in moist air. A corresponding molybdenum iodide compound is also employed.

Results and discussion

Several routes have been reported to synthesize ternary tungsten iodides.^{21–23} A limiting step in the synthesis of ligand-substituted cluster compounds is the transformation of insoluble $\text{Cs}_2[\text{W}_6\text{I}_8\text{I}_6]$ into the soluble precursor $(\text{TBA})_2[\text{W}_6\text{I}_8\text{I}_6]$ by cation exchange, because this step does not proceed in solution but from a slurry of $\text{Cs}_2[\text{W}_6\text{I}_8\text{I}_6]$ powder.²⁴ $(\text{TBA})_2[\text{W}_6\text{I}_8\text{I}_6]$ is then reacted with a corresponding silver salt (*e.g.* $\text{Ag}(\text{C}_7\text{H}_7\text{SO}_3)$, $\text{Ag}(\text{COOCF}_3)$, *etc.*) to replace the six terminal iodido ligands to yield $(\text{TBA})_2[\text{W}_6\text{I}_8\text{L}_6]$ (Fig. 1). Following a new reactions strategy we have employed soluble W_6I_{22} ²⁵ instead of $\text{Cs}_2[\text{W}_6\text{I}_{14}]$, allowing for a higher reaction rate and a high volume synthesis (≥ 5 g) of $(\text{TBA})_2[\text{W}_6\text{I}_8\text{L}_6]$ and finally the ligand-substituted cluster.

The luminescence spectrum of such microcrystalline $(\text{TBA})_2[\text{W}_6\text{I}_8(\text{C}_7\text{H}_7\text{SO}_3)_6]$ exhibits a broad emission band at 678 nm (1.83 eV) from excited spin triplet states upon excitation with 400 nm radiation. The phosphorescence is quenched in the presence of oxygen. Hence, the phosphorescence intensity as well as the decay time decrease with increasing oxygen partial pressure. The decay time of $(\text{TBA})_2[\text{W}_6\text{I}_8(\text{C}_7\text{H}_7\text{SO}_3)_6]$ in pure nitrogen is 24 μs and in pure oxygen 11.9 μs . Similar properties are observed for $(\text{TBA})_2[\text{W}_6\text{I}_8(\text{CF}_3\text{COO})_6]$ with a maximum emission at 660 nm (1.88 eV) and luminescence lifetimes of 29.2 μs and 9.9 μs . The corresponding molybdenum species $(\text{TBA})_2[\text{Mo}_6\text{I}_8(\text{C}_7\text{H}_7\text{SO}_3)_6]$ shows an emission band at 676 nm (1.83 eV) and decay times of 147 μs and 64 μs in nitrogen and pure oxygen atmosphere.

Encapsulation of $\text{A}_2[\text{M}_6\text{I}_8\text{L}_6]$ into silicone

Molybdenum and tungsten clusters of the type $\text{A}_2[\text{M}_6\text{I}_8\text{L}_6]$ are insoluble in water and tend to hydrolyse in a humid environment. Therefore, for a possible application outside and inside medical applications the compounds either have to be equipped with an appropriate ligand or incorporated into a carrier.

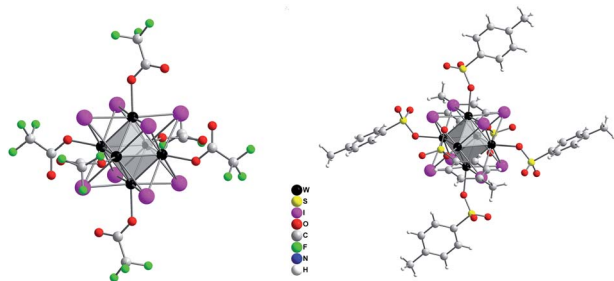


Fig. 1 View of used cluster anions $[\text{W}_6\text{I}_8(\text{COOCF}_3)_6]^{2-}$ (left) and $[\text{W}_6\text{I}_8(\text{C}_7\text{H}_7\text{SO}_3)_6]^{2-}$ (right).

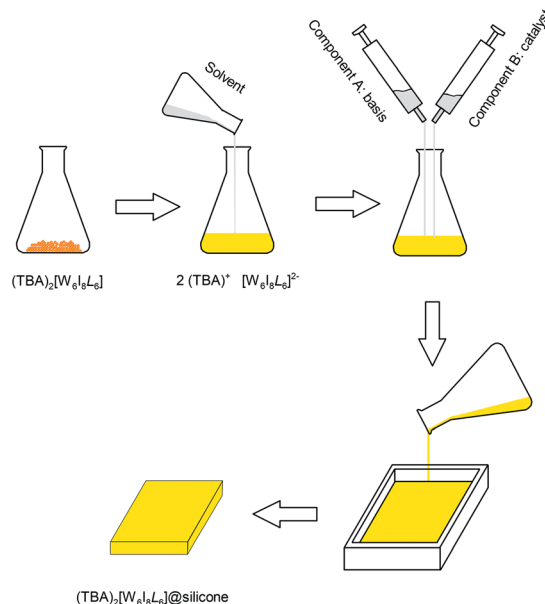


Fig. 2 Procedure for the incorporation of $(\text{TBA})_2[\text{W}_6\text{I}_8\text{L}_6]$ into silicone.

There are different approaches already described, the incorporation into functionalized polystyrene (PS-SH, PS-Py, PS-COOH) microspheres^{26–28} where the labile NO_3^- ligand is substituted for a polymer matrix or for biological applications into mitochondrion²⁹ to prevent degeneration. In case of $[\text{Mo}_6\text{I}_8@\text{PS-SH}]$, however, this compound does not show luminescence quenching by neither solvent nor oxygen and therefore no singlet oxygen generation. Another approach is the incorporation into fluorinated matrices to increase oxygen diffusion and therefore singlet oxygen production.²⁹ Since we are aiming for biological applications we incorporated the cluster compounds into a silicone matrix (Fig. 2), thereby maintaining the production of singlet oxygen, to measure the dark- and photo-induced antibacterial and antifungal activities of these materials.

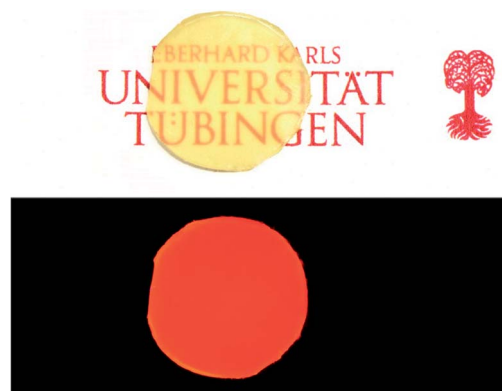


Fig. 3 Photograph of a circular cut silicone disc (adopted from Fig. 2) implanted with $(\text{TBA})_2[\text{W}_6\text{I}_8(\text{C}_7\text{H}_7\text{SO}_3)_6]$ under daylight (top) and under UV irradiation (bottom, 366 nm).



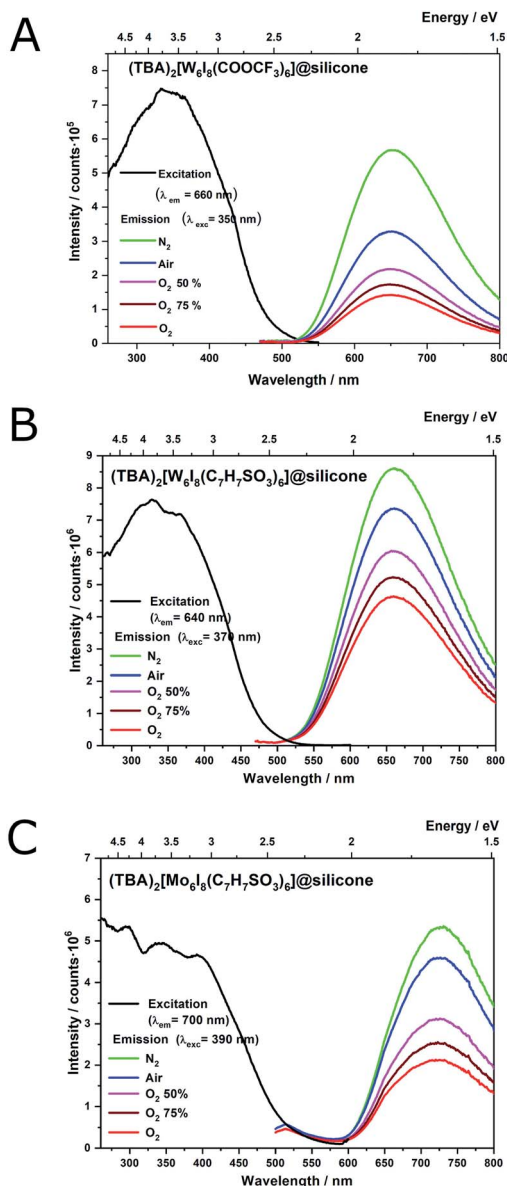


Fig. 4 Excitation and emission spectra of $(\text{TBA})_2[\text{W}_6\text{I}_8(\text{COOCF}_3)_6]$ (A), $(\text{TBA})_2[\text{W}_6\text{I}_8(\text{C}_7\text{H}_7\text{SO}_3)_6]$ (B), and $(\text{TBA})_2[\text{Mo}_6\text{I}_8(\text{C}_7\text{H}_7\text{SO}_3)_6]$ (C) encapsulated into silicone, recorded under various O_2 partial pressures, ranging from 0 mbar O_2 (in N_2) to 1013 mbar O_2 (pure O_2).

Dimethyl silicone is one of the permeable elastomers available.³⁰ Common usage for this kind of polymer are in blood oxygenation, gas separation and drug delivery.³¹ We use a common available two component RTV silicone (room temperature vulcanization) which offers great oxygen permeability due to the high flexibility of the oxygen-silicone chains which create openings and holes in the matrix for gas diffusion ($570 \text{ cm}^3 \text{ mm m}^{-2} \text{ h}^{-1} \text{ bar}^{-1}$ at room temperature). However, this flexibility is dependent on the polarity of the residues attached to the Si-O skeleton, in the latter case methyl. As a catalyst for the polymerization, either a diacetyl peroxide or acetic acid is used. In our case a platinum cross-linker is used, which is common especially in medical products because they produce less unwanted side products.³² Another advantage of

elastomers is the fact that it is possible to create almost any imaginable shapes. The respective cluster compound was incorporated by dissolution in dichloromethane under dissociation into TBA^+ ions and $[\text{M}_6\text{I}_8\text{L}_6]^{2-}$ clusters. Solidification of the matrix starts on adding the second component (see Experimental section). Fig. 3 shows an example of $(\text{TBA})_2[\text{W}_6\text{I}_8(\text{C}_7\text{H}_7\text{SO}_3)_6]$ incorporated into silicone.

Luminescence of $\text{A}_2[\text{M}_6\text{I}_8\text{L}_6]$ @silicone

Clusters incorporated into silicone ($\text{A}_2[\text{M}_6\text{I}_8\text{L}_6]$ @silicone) show similar broad excitation and emission bands as in solid state or solution. Crystalline samples of ligand substituted compounds $[\text{W}_6\text{I}_8\text{L}_6]^{2-}$ show luminescence quenching rates in the order of 50% for $\text{L} = \text{tosylate}$ and 66% for $\text{L} = \text{trifluoroacetate}$ (Fig. 4A and B).^{10,33} The dependency of the emission, *i.e.* luminescence quenching rate with the oxygen partial pressure can be regarded as a measure for the singlet oxygen production rate. The recorded spectra of clusters incorporated into silicone are showing only smaller deviations to those of the respective crystalline powders (36% and 57%, respectively). Monitored phosphorescence quantum yields (Φ_p) tend to increase in case of $(\text{TBA})_2[\text{W}_6\text{I}_8(\text{C}_7\text{H}_7\text{SO}_3)_6]$ from 0.028 in solution to 0.14 @silicone and for $(\text{TBA})_2[\text{W}_6\text{I}_8(\text{COOCF}_3)_6]$ from 0.015 in solution to 0.21 @silicone. This is not unexpected because it has been shown that oxygen quenching is always more efficient in solution. $(\text{TBA})_2[\text{Mo}_6\text{I}_8(\text{C}_7\text{H}_7\text{SO}_3)_6]$ did not show a significant difference in the quantum yield after being incorporated into silicone.

The photoluminescence spectrum of $(\text{TBA})_2[\text{Mo}_6\text{I}_8(\text{C}_7\text{H}_7\text{SO}_3)_6]$ @silicone (Fig. 4C) shows a significant shift in the emission maximum. While a maximum emission is expected at around 660 to 670 nm for $(\text{TBA})_2[\text{Mo}_6\text{I}_8(\text{C}_7\text{H}_7\text{SO}_3)_6]$, a red shift towards 731 nm is observed. The lifetimes of excited states decrease from 147 μs (solid state) to 47 μs (@silicone), suggesting some kind of transformation of the cluster compound. This finding is most likely due to hydrolysis of the cluster, respectively substitution of terminal ligands to yield aqua hydroxo complexes, as has been described in previous literature.³⁴ This degradation is significantly faster in the case of molybdenum compared to tungsten cluster compounds.³⁴ The same behaviour is likely here in the sense that the clusters@silicone are “diluted” into the silicone matrix which contains traces of oxygen and water and is furthermore permeable for small molecules and gases.³⁰ Hydrolysed and aqua complexes tend to show a significant decrease in phosphorescence intensity (due to non-radiative deactivation by water), including a red shift in the emission spectrum.¹⁷ Luminescence spectra of tungsten compounds remained more or less the same in solid state, solution and in silicone (Table 1).

Antibacterial and antifungal studies of the silicone materials

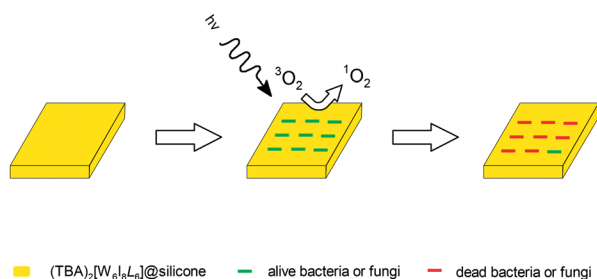
An evaluation of antimicrobial photodynamic inactivation (PDI)³⁶ activity on the surface of the neat silicone and the cluster-doped materials on Gram-negative *E. coli*, *S. typhimurium*, *P. aeruginosa* and on Gram-positive *S. aureus* bacteria was investigated. Also, an antifungal photodynamic inactivation activity on *C. albicans* fungi was evaluated.



Table 1 Luminescence properties of $(\text{TBA})_2[\text{W}_6\text{I}_8(\text{C}_7\text{H}_7\text{SO}_3)_6]$, $(\text{TBA})_2[\text{Mo}_6\text{I}_8(\text{C}_7\text{H}_7\text{SO}_3)_6]$ and $(\text{TBA})_2[\text{W}_6\text{I}_8(\text{COOCF}_3)_6]$ in solid state, in solution, and after incorporation into silicone

	Emission maximum in/nm	$\tau_{1/2}/\mu\text{s}$				Φ_{P}
Compound	Powder	Pure N ₂	Air	Pure O ₂	N ₂ /O ₂ ^a quenching	Air
(TBA)₂[W₆I₈(COOCF₃)₆]						
In solid state ¹⁰	660	29.2		9.9	66.1%	0.04
In solution ¹⁰	677	36	1.08	0.23	99.4%	0.015
@silicone	651	30.2		12.9	57.3%	0.21
(TBA)₂[W₆I₈(C₇H₇SO₃)₆]						
In solid state ³³	678	24		11.9	50.4%	
In solution ³³	675	40.2	1.94	0.91	97.7%	0.028
@silicone	660	28	24	18	35.7%	0.14
(TBA)₂[Mo₆I₈(C₇H₇SO₃)₆]						
In solid state ³⁵	676	147	111	64	56.5%	
In solution ³⁵	671	232	4.94	2.11	99.1%	0.011
@silicone	731	47	38	27	42.6%	0.02

^a N_2/O_2 quenching: luminescence quenching when switching the atmosphere from N_2 to O_2 .

**Fig. 5** Schematic overview of the antibacterial properties of cluster@silicone.

Microorganism-infected samples were then irradiated with a white spot-light source (400–800 nm) for 10 min (Fig. 5). Data obtained (Table 2) shows that $(\text{TBA})_2[\text{W}_6\text{I}_8(\text{COOCF}_3)_6]$ @silicone and $(\text{TBA})_2[\text{W}_6\text{I}_8(\text{C}_7\text{H}_7\text{SO}_3)_6]$ @silicone exhibit noticeable light-induced antimicrobial activity, while $(\text{TBA})_2[\text{Mo}_6\text{I}_8(\text{C}_7\text{H}_7\text{SO}_3)_6]$ @silicone and neat silicone have very slight activity against a negative control *i.e.* neat silicon that was not exposed to light. Since the luminescence quenching by oxygen for $(\text{TBA})_2[\text{W}_6\text{I}_8(\text{COOCF}_3)_6]$ (57.3%) is highest among investigated, $(\text{TBA})_2[\text{Mo}_6\text{I}_8(\text{C}_7\text{H}_7\text{SO}_3)_6]$ (42.6%) and

$(\text{TBA})_2[\text{W}_6\text{I}_8(\text{C}_7\text{H}_7\text{SO}_3)_6]$ (35.7%), is assumed that the PDI efficacy has the same order. However, it was unexpected that the PDI efficacy for $(\text{TBA})_2[\text{W}_6\text{I}_8(\text{C}_7\text{H}_7\text{SO}_3)_6]$ @silicone was higher than for others, while molybdenum one has worst PDI activity. The possible reason of this behaviour could be the difference in the singlet oxygen lifetime due to the different self-quenching effect that was previously demonstrated on the hexacyanido rhenium cluster complexes.³⁷ Moreover, it was previously reported that octahedral iodide tungsten cluster complexes $[\text{W}_6\text{I}_8\text{L}_6]^{2-}$ under illumination can produce not only singlet oxygen but also superoxide ion O_2^- .³⁸ Such reactive oxygen radical has significantly higher lifetime than singlet oxygen (minutes *vs.* microseconds in aqueous media),^{39,40} and hence may have a longer effect on microorganisms.

These both possibilities may be the reason for such a low PDI activity for molybdenum material $(\text{TBA})_2[\text{Mo}_6\text{I}_8(\text{C}_7\text{H}_7\text{SO}_3)_6]$ @silicone that comparable to PDI for the neat silicone. The presented data for bacterial cultures is in good agreement with earlier reported for cluster-doped fluoroplast F-32L²⁹ *i.e.* the most resistant microorganisms are Gram-positive *S. aureus* and Gram-negative *P. aeruginosa*. Nevertheless, $(\text{TBA})_2[\text{W}_6\text{I}_8(\text{C}_7\text{H}_7\text{SO}_3)_6]$ @silicone demonstrated significant PDI activity even for *S. aureus* and *P. aeruginosa* with a microorganisms proliferation inhibition up to

Table 2 The percentage of colony-forming units in comparison to control for the cluster doped silicon after irradiation with a white light source. The confidence interval is calculated for $P = 0.95$

Sample	<i>S. aureus</i>	<i>E. coli</i>	<i>S. typhimurium</i>	<i>P. aeruginosa</i>	<i>C. albicans</i> (Fungi)
Negative control	100 ± 7	100 ± 6	100 ± 8	100 ± 11	100 ± 3
Neat silicone	89.9 ± 7.1	99.4 ± 3.9	93.1 ± 4.8	88.0 ± 4.4	82.5 ± 6.8
$(\text{TBA})_2[\text{W}_6\text{I}_8(\text{COOCF}_3)_6]$ @silicone	17.8 ± 2.4	1.7 ± 0.3	1.09 ± 0.05	9.2 ± 0.9	4.6 ± 0.5
$(\text{TBA})_2[\text{W}_6\text{I}_8(\text{C}_7\text{H}_7\text{SO}_3)_6]$ @silicone	0.89 ± 0.09	0.8 ± 0.1	0.93 ± 0.05	2.1 ± 0.4	2.6 ± 0.2
$(\text{TBA})_2[\text{Mo}_6\text{I}_8(\text{C}_7\text{H}_7\text{SO}_3)_6]$ @silicone	99.7 ± 4.5	90.2 ± 9.8	83.6 ± 4.8	67.6 ± 8.5	90.5 ± 5.4



98%. The data of antifungal PDI activity on cluster-based materials are presented for the first time.

Conclusions

(TBA)₂[W₆I₈L₆] cluster compounds are known for their photo-physical properties including their activity as efficient singlet oxygen sensitizers with atmospheric oxygen. The employment of singlet oxygen as a residue-free agent in the neutralization of bacteria, fungi or even viruses is a great challenge.

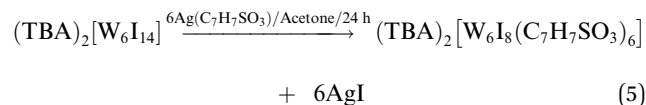
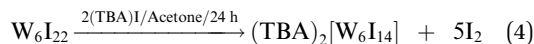
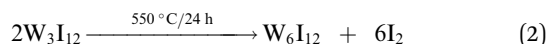
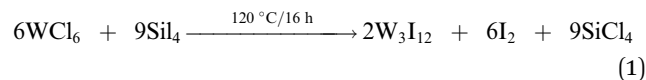
Cluster compounds under consideration belong to the small group of inorganic singlet oxygen sensitizers which remain widely intact in the presence of singlet oxygen, compared to the multitude of organic counterparts. Within the current exploration we implanted cluster compounds into a silicon basin to explore their light-induced antimicrobial activity. Composite (TBA)₂[W₆I₈L₆]@silicon materials are showing good chemical and photochemical stabilities with similar properties as their respective crystalline powders. (TBA)₂[W₆I₈(COOCF₃)₆]@silicone and (TBA)₂[W₆I₈(C₇H₇SO₃)₆]@silicone exhibit high light-induced antimicrobial activity against the sections of bacteria including multi-resistant hospital germs such as *S. aureus* and *P. aeruginosa* as well as fungi. The somewhat lower efficiency of (TBA)₂[W₆I₈(COOCF₃)₆]@silicone could be attributed to a longer singlet oxygen lifetime.

Experimental Section

The preparation and structural characterization of (TBA)₂[W₆I₈(C₇H₇SO₃)₆]³³, (TBA)₂[Mo₆I₈(C₇H₇SO₃)₆]^{33,41} and (TBA)₂[W₆I₈(COOCF₃)₆]¹⁰ were already reported. Herein we present a high-volume synthesis for tungsten iodide phosphors with the [W₆I₈]-core, departing from W₆I₂₂ instead of Cs₂[W₆I₁₄]. W₆I₂₂ was prepared according to the literature.^{1,42} Purities of products from individual reaction steps were explored by means of X-ray powder diffraction. W₆I₂₂ was obtained in a high-volume synthesis for the first time in high purity (see ESI†). The identity of compounds obtained therefrom, (TBA)₂[W₆I₈(C₇H₇SO₃)₆] and (TBA)₂[W₆I₈(COOCF₃)₆] was proven by comparison with single crystal data from literature and ESI-MS measurements.

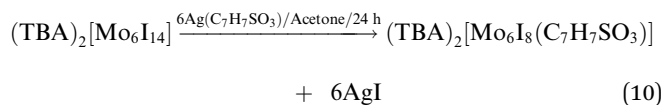
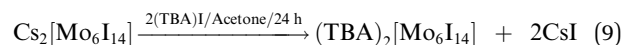
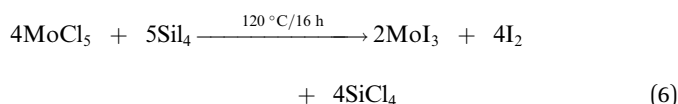
Synthesis of (TBA)₂[W₆I₈L₆] with L = C₇H₇SO₃, COOCF₃

W₆I₂₂ (5 g, 1.28 mmol) was dissolved in acetone (100 ml, HPLC grade) and (TBA)I (0.47 g, 1.28 mmol) was added under air. The solution was stirred for one day and the solvent was left to evaporate at room temperature. The product was obtained as a dark green powder. Traces of iodine can be separated by column chromatography to obtain an orange powder.⁴³ Ligand exchange reactions were performed by exchanging the terminal cluster ligands by adding silver *p*-toluene sulfonate or silver trifluoroacetate, respectively, according to the following equation on the example of (TBA)₂[W₆I₈(C₇H₇SO₃)₆].^{33,41} All reactions (1–5) proceed in high yields (>95%).



Synthesis of (TBA)₂[Mo₆I₈L₆] with L = C₇H₇SO₃

The synthesis was carried out according to literature³³ procedure starting from a halide exchange with MoCl₅ and SiI₄ according to the following equations on the example of (TBA)₂[W₆I₈(C₇H₇SO₃)₆].^{33,41,44} All reactions (6–10) proceed in high yields (>95%).



Synthesis of cluster@silicone composites

The silicone matrix was prepared from a commercial room temperature vulcanization silicone (RTV2 silicone SF33). Typically, 4 mg of (TBA)₂[M₆I₈L₆] with M = Mo, W and L = C₇H₇SO₃, COOCF₃ was dissolved into 1 ml dichloromethane (solution A). Solution A was mixed with 2 ml component basis and 2 ml component catalyst of silicone. The mixture was placed into a homemade casting box and slowly evacuated for 5–10 minutes to remove air bubbles from silicone. After 24 h the composite was removed. All silicone discs of A₂[M₆I₈L₆]@silicone appeared transparent with a yellow body colour (Fig. 3) typically obtained for the diluted solid (ground with BaSO₄), or dissolved cluster compound.

Tungsten iodide clusters in silicone show very good stability. The maximum emission observed for (TBA)₂[W₆I₈(C₇H₇SO₃)₆]@silicone only shifts within the error of the measurement, from 660 nm (1.88 eV) to 662 nm (1.87 eV) after six months. In the same timeframe the maximum emission of (TBA)₂[Mo₆I₈(C₇H₇SO₃)₆]@silicone shows a shift from 731 nm (1.70 eV) to 744 nm (1.67 eV) indicating an ongoing hydrolysis of the compound.



Luminescence measurements

Excitation and emission spectra on $(\text{TBA})_2[\text{M}_6\text{I}_8\text{L}_6]@\text{silicone}$ with $\text{M} = \text{Mo}, \text{W}$ and $\text{L} = \text{C}_7\text{H}_7\text{SO}_3, \text{COOCF}_3$ were collected with a fluorescence spectrometer FLS920 (Edinburgh Instruments) equipped with a 450 W ozone-free xenon discharge lamp (OSRAM) and a cryostat "MicrostatN" from Oxford Instruments sample chamber installed with a mirror optic for powder samples. For detection, an R2658P single-photon-counting photomultiplier tube (Hamamatsu) was used. All luminescence spectra were recorded with a spectral resolution of 1 nm, a dwell time of 0.4 s in 1 nm steps and 3 repeats. Quantum yields were measured according to Yuichiro Kawamura⁴⁵ upon excitation of 450 nm, 3 nm spectral resolution, while respective emission intensity from 420 nm to 870 nm with a spectral resolution of 0.5 nm with 0.5 nm steps was recorded.

Photodynamic inactivation

The antibacterial and antifungal photodynamic inactivation activity of the materials on *Escherichia coli* (ATCC25922), *Staphylococcus aureus* (ATCC25923), *Salmonella typhimurium* (ATCC14028) and *Pseudomonas aeruginosa* (ATCC27853) bacteria, and *Candida albicans* (ATCC10231) fungi was tested. The bacteria and fungi were cultivated in Lysogeny broth (LB) medium at 37 °C. Microorganisms diluted in saline at concentrations of $1\text{--}1.2 \times 10^6$ CFU ml^{-1} (CFU – colony-forming units) were used in the experiments. The number of viable microorganisms was estimated *via* counting of the colony-forming units (CFU) after 24 h of cultivation. All experiments were performed in triplicate with a confidence interval for $P = 0.95$.

All samples were cut into strips with lateral size of 0.5 cm \times 2.0 cm. The strips were coated into a solution with microorganisms, then they were placed on a dry surface of the Petri dishes and irradiated with a spot light source L8253 (Hamamatsu) at a distance of 20 cm for 10 min (400–800 nm, 220 mW cm^{-2}) for each side, *i.e.* the strips were transferred to a new dry dish and turned over to process the second side. For the negative control, all the procedures were similarly performed, but the coated strips were kept in the dark for the same time. After irradiation, strips were placed into test tubes and suspended with 1000 μL of saline for 1 min. 1000 μL of the culture media was collected from the test tube and cultivated in LB agar culture media. The number of colonies were counted after 24 h. Fig S5† shows images of the microorganisms' growth in LB agar culture media.

Electron spray ionisation (ESI) measurements

All ESI-MS measurements were performed on a Bruker Esquire 3000 plus Ion Trap LC/MS system in positive mode in methanol solution. ESI-MS: $(\text{TBA})_2[\text{W}_6\text{I}_8(\text{CF}_3\text{COO})_6]$ revealed $m/z = 3037.6$ for $(\text{TBA})[\text{W}_6\text{I}_8(\text{CF}_3\text{COO})_6]^-$; theoretical values: $m/z = 3038.8$ for $(\text{TBA})[\text{W}_6\text{I}_8(\text{CF}_3\text{COO})_6]^-$. ESI-MS: $(\text{TBA})_2[\text{W}_6\text{I}_8(\text{C}_7\text{H}_7\text{SO}_3)_6]$ revealed $m/z = 1572.8$ for $[\text{W}_6\text{I}_8(\text{O}_3\text{SC}_7\text{H}_7)_6]^{2-}$; theoretical values: $m/z = 1572.7$ for $[\text{W}_6\text{I}_8(\text{O}_3\text{SC}_7\text{H}_7)_6]^{2-}$.

Conflicts of interest

There are no conflicts to declare.

Acknowledgements

This work was supported by the Russian Foundation for Basic Research (grant number 19-53-12019) and the Deutsche Forschungsgemeinschaft (grant number ME914-31-1).

Notes and references

- 1 M. Ströbele and H.-J. Meyer, *Dalton Trans.*, 2019, **48**, 1547–1561.
- 2 D. Bublit, W. Preetz and M. K. Simsek, *Z. Anorg. Allg. Chem.*, 1997, **623**, 1–7.
- 3 M. N. Sokolov, M. A. Mihailov, E. V. Peresypkina, K. A. Brylev, N. Kitamura and V. P. Fedin, *Dalton Trans.*, 2011, **40**, 6375–6377.
- 4 M. N. Sokolov, M. A. Mikhailov, K. A. Brylev, A. V. Virovets, C. Vicent, N. B. Kompankov, N. Kitamura and V. P. Fedin, *Inorg. Chem.*, 2013, **52**, 12477–12481.
- 5 K. Kirakci, K. Fejfarova, M. Kucerakova and K. Lang, *Eur. J. Inorg. Chem.*, 2014, **2014**, 2331–2336.
- 6 O. A. Efremova, M. A. Shestopalov, N. A. Chirtsova, A. I. Smolentsev, Y. V. Mironov, N. Kitamura, K. A. Brylev and A. J. Sutherland, *Dalton Trans.*, 2014, **43**, 6021–6025.
- 7 O. A. Efremova, Y. A. Vorotnikov, K. A. Brylev, N. A. Vorotnikova, I. N. Novozhilov, N. V. Kuratieva, M. V. Edeleva, D. M. Benoit, N. Kitamura, Y. V. Mironov, M. A. Shestopalov and A. J. Sutherland, *Dalton Trans.*, 2016, **45**, 15427–15435.
- 8 M. A. Mikhailov, K. A. Brylev, P. A. Abramov, E. Sakuda, S. Akagi, A. Ito, N. Kitamura and M. N. Sokolov, *Inorg. Chem.*, 2016, **55**, 8437–8445.
- 9 M. A. Mikhaylov and M. A. Sokolov, *Eur. J. Inorg. Chem.*, 2019, **2019**, 4181–4197.
- 10 L. Riehl, A. Seyboldt, M. Ströbele, D. Ensling, T. Jüstel, M. Westberg, P. R. Ogilby and H.-J. Meyer, *Dalton Trans.*, 2016, **45**, 15500–15506.
- 11 A. U. Khan and M. Kasha, *J. Chem. Phys.*, 1963, **39**, 2105–2106.
- 12 D. J. Osborn, G. L. Baker and R. N. Ghosh, *J. Sol-Gel Sci. Technol.*, 2005, **36**, 5–10.
- 13 R. N. Ghosh, P. A. Askeland, S. Kramer and R. Loloee, *Appl. Phys. Lett.*, 2011, **98**, 221103.
- 14 T. C. Zietlow, D. G. Nocera and H. B. Gray, *Inorg. Chem.*, 1986, **25**, 1351–1353.
- 15 K. Kirakci, P. Kubat, M. Kucerakova, V. Sicha, H. Gbelcova, P. Lovecka, P. Grznarova, T. Ruml and K. Lang, *Inorg. Chim. Acta*, 2016, **441**, 42–49.
- 16 A. Barras, S. Cordier and R. Boukherroub, *Appl. Catal., B*, 2012, **123**, 1–8.
- 17 D. V. Evtushok, A. R. Melnikov, N. A. Vorotnikova, Y. A. Vorotnikov, A. A. Ryadun, N. V. Kuratieva, K. V. Kozyr, N. R. Obedinskaya, E. I. Kretov, I. N. Novozhilov, Y. V. Mironov, D. V. Stass, O. A. Efremova and M. A. Shestopalov, *Dalton Trans.*, 2017, **46**, 11738–11747.
- 18 M. Feliz, M. Puche, P. Atienzar, P. Concepcion, S. Cordier and Y. Molard, *ChemSusChem*, 2016, **9**, 1963–1971.



- 19 P. Kumar, S. Kumar, S. Cordier, S. Paofai, R. Boukherroub and S. L. Jain, *RSC Adv.*, 2014, **4**, 10420–10423.
- 20 K. Kirakci, J. Zelenka, M. Rumlova, J. Cvacka, T. Ruml and K. Lang, *Biomater. Sci.*, 2019, **7**, 1386–1392.
- 21 J. D. Franolic, J. R. Long and R. H. Holm, *J. Am. Chem. Soc.*, 1995, **117**, 8139–8153.
- 22 M. A. Riche, *Ann. Chim. Phys.*, 1857, **3**, 5.
- 23 A. D. Westland and N. Muriithi, *Inorg. Chem.*, 1973, **12**, 2356–2361.
- 24 T. Hummel, M. Ströbele, D. Schmid, D. Enseling, T. Jüstel and H.-J. Meyer, *Eur. J. Inorg. Chem.*, 2016, **2016**, 5063–5067.
- 25 H. Schäfer and H. G. Schulz, *Z. Anorg. Allg. Chem.*, 1984, **516**, 196–200.
- 26 K. Kirakci, P. Kubat, K. Fejfarova, J. Martincik, M. Nikl and K. Lang, *Inorg. Chem.*, 2016, **55**, 803–809.
- 27 N. A. Vorotnikova, M. V. Edeleva, O. G. Kurskaya, K. A. Brylev, A. M. Shestopalov, Y. V. Mironov, A. J. Sutherland, O. A. Efremova and M. A. Shestopalov, *Polym. Int.*, 2017, **66**, 1906–1912.
- 28 N. A. Vorotnikova, O. A. Efremova, A. R. Tsygankova, K. A. Brylev, M. V. Edeleva, O. G. Kurskaya, A. J. Sutherland, A. M. Shestopalov, Y. V. Mironov and M. A. Shestopalov, *Polym. Adv. Technol.*, 2016, **27**, 922–928.
- 29 N. A. Vorotnikova, A. Y. Alekseev, Y. A. Vorotnikov, D. V. Evtushok, Y. Molard, M. Amela-Cortes, S. Cordier, A. I. Smolentsev, C. G. Burton, P. M. Kozhin, P. Zhu, P. D. Topham, Y. V. Mironov, M. Bradley, O. A. Efremova and M. A. Shestopalov, *Mater. Sci. Eng., C*, 2019, **105**, 110150.
- 30 W. L. Robb, *Ann. N. Y. Acad. Sci.*, 1968, **146**, 119–137.
- 31 E. L. Warrick, O. R. Pierce, K. E. Polmanteer and J. C. Saam, *Rubber Chem. Technol.*, 1979, **52**, 437–525.
- 32 L. N. Lewis, J. Stein, Y. Gao, R. E. Colborn and G. Hutchins, *Platinum Met. Rev.*, 1997, **41**, 66–75.
- 33 A. Seyboldt, D. Enseling, T. Jüstel, M. Ivanovic, H. Peisert, T. Chasse and H.-J. Meyer, *Eur. J. Inorg. Chem.*, 2017, **2017**, 5387–5394.
- 34 E. V. Svezhentseva, Y. A. Vorotnikov, A. O. Solovieva, T. N. Pozmogova, I. V. Eltssov, A. A. Ivanov, D. V. Evtushok, S. M. Miroshnichenko, V. V. Yanshole, C. J. Eling, A. M. Adawi, J. S. G. Bouillard, N. V. Kuratieva, M. S. Fufaeva, L. V. Shestopalova, Y. V. Mironov, O. A. Efremova and M. A. Shestopalov, *Chem.-Eur. J.*, 2018, **24**, 17915–17920.
- 35 M. A. Mikhailov, A. L. Gushchin, M. R. Gallyamov, A. V. Virovets, M. N. Sokolov, D. G. Sheven and V. V. Pervukhin, *Russ. J. Coord. Chem.*, 2017, **43**, 172–180.
- 36 M. R. Hamblin, *Curr. Opin. Microbiol.*, 2016, **33**, 67–73.
- 37 A. O. Solovieva, K. Kirakci, A. A. Ivanov, P. Kubat, T. N. Poznaogova, S. M. Miroshnichenko, E. V. Vorontsova, A. V. Chechushkov, K. E. Trifonova, M. S. Fufaeva, E. I. Kretov, Y. V. Mironov, A. F. Poveshchenko, K. Lang and M. A. Shestopalov, *Inorg. Chem.*, 2017, **56**, 13491–13499.
- 38 J. A. Jackson, C. Turro, M. D. Newsham and D. G. Nocera, *J. Phys. Chem.*, 1990, **94**, 4500–4507.
- 39 M. Hayyan, M. A. Hashim and I. M. AlNashef, *Chem. Rev.*, 2016, **116**, 3029–3085.
- 40 E. Appiani, R. Ossola, D. E. Latch, P. R. Erickson and K. McNeill, *Environ. Sci.: Process. Impacts*, 2017, **19**, 507–516.
- 41 A.-D. Fuhrmann, A. Seyboldt, A. Schank, G. Zitzer, B. Speiser, D. Enseling, T. Jüstel and H.-J. Meyer, *Eur. J. Inorg. Chem.*, 2017, **2017**, 4259–4266.
- 42 M. Ströbele and H.-J. Meyer, *Inorg. Chem.*, 2019, **58**, 12867–12872.
- 43 T. Hummel, M. Ströbele, A. D. Fuhrmann, D. Enseling, T. Jüstel and H.-J. Meyer, *Eur. J. Inorg. Chem.*, 2019, **2019**, 4014–4019.
- 44 M. Ströbele, R. Thalwitzer and H.-J. Meyer, *Inorg. Chem.*, 2016, **55**, 12074–12078.
- 45 Y. Kawamura, H. Sasabe and C. Adachi, *Jpn. J. Appl. Phys.*, 2004, **43**, 7729–7730.

